

# Significant low lattice thermal conductivity and potential high thermoelectric figure of merit in $\text{Na}_2\text{MgSn}$

Cong Wang<sup>1</sup>, Y. B. Chen<sup>2</sup>, Shu-Hua Yao<sup>1</sup>, and Jian Zhou<sup>1,3\*</sup>

<sup>1</sup> *National Laboratory of Solid State Microstructures and Department of Materials Science and Engineering, Nanjing University, Nanjing 210093, China*

<sup>2</sup> *National Laboratory of Solid State Microstructures and Department of Physics, Nanjing University, Nanjing 210093, China*

<sup>3</sup> *Collaborative Innovation Center of Advanced Microstructures, Nanjing University, Nanjing , 210093, China.*

(Dated: November 29, 2021)

## Abstract

Thermoelectric materials enables the harvest of waste heat and directly conversion into electricity. In search of high efficient thermoelectric materials, low thermal conductivity of a material is essential and critical. Here, we have theoretically investigated the lattice thermal conductivity and thermoelectric properties of layered intermetallic  $\text{Na}_2\text{MgSn}$  and  $\text{Na}_2\text{MgPb}$  based on the density functional theory and linearized Boltzmann equation with the single-mode relaxation-time approximation. It is found that both materials exhibit very low and anisotropic intrinsic lattice thermal conductivity. Despite of the very low mass density and simple crystal structure of  $\text{Na}_2\text{MgSn}$ , its lattice thermal conductivities along  $a$  and  $c$  axes are only 1.75 and 0.80 W/m·K respectively at room temperatures. When Sn is replaced by the heavier element Pb, its lattice thermal conductivities decrease remarkably to 0.51 and 0.31 W/m·K respectively along  $a$  and  $c$  axes at room temperatures. We show that the low lattice thermal conductivities of both materials are mainly due to their very short phonon lifetimes, which are roughly between 0.4 to 4.5 ps. Combined with previous experimental measurements, the metallic  $\text{Na}_2\text{MgPb}$  can not be a good thermoelectric material. However, we predict that the semiconducting  $\text{Na}_2\text{MgSn}$  is a potential room-temperature thermoelectric material with a considerable  $ZT$  of 0.34 at 300 K. Our calculations not only imply that the intermetallic  $\text{Na}_2\text{MgSn}$  is a potential thermoelectric material, but also can motivate more theoretical and experimental works on the thermoelectric researches in simple layered intermetallic compounds.

PACS numbers:

---

\*Corresponding author: zhoujian@nju.edu.cn

## I. INTRODUCTION

Thermoelectrical (TE) materials, which can directly convert heat to electricity, have been extensively studied for last several decades since they play an important role in the area of environmentally friendly energy technology. [1, 2] The conversion efficiency of TE materials is usually evaluated by a dimensionless figure of merit,  $ZT = S^2\sigma T/\kappa$ , where  $S$ ,  $\sigma$ ,  $T$ , and  $\kappa$  are the Seebeck coefficient, electrical conductivity, absolute temperature and thermal conductivity respectively. The thermal conductivity  $\kappa$  of a material can be further divided into two items:  $\kappa = \kappa_e + \kappa_L$ , where  $\kappa_e$  and  $\kappa_L$  are electronic and lattice thermal conductivity respectively. For practical applications, the  $ZT$  of a TE material should be at least larger than 1. To be competitive, a higher  $ZT$  of 4 is needed.[3] However, these physical quantities ( $S$ ,  $\sigma$ , and  $\kappa$ ) in the same material can not be tuned separately due to their internal relationship. In general, the electrical conductivity ( $\sigma$ ) and electronic thermal conductivity ( $\kappa_e$ ) will increase with the increase of carrier concentration, while the Seebeck coefficient ( $S$ ) will decrease with it. [1] Therefore, most good TE materials are semiconductors, such as IV-VI compounds PbTe [4] and SnSe. [5, 6]

On the other hand, the lattice thermal conductivity ( $\kappa_L$ ) is not directly related to the carrier concentration. It is an effective method to tune the  $ZT$  values of materials by tuning their lattice thermal conductivities. Typical materials with low lattice thermal conductivities are glasses. However, glasses are bad TE materials because of their very low carrier concentration and mobility compared with crystalline semiconductors. [1] Therefore, good TE materials require a rather peculiar property in the same system: ‘phonon-glass electron-crystal’. [7] In other words, low lattice thermal conductivity is a necessary condition for good TE materials, although not a sufficient one.

In the classic physics picture, the lattice thermal conductivity can be approximated by the formula:  $\kappa_L = \frac{1}{3}C_vvl = \frac{1}{3}C_vv^2\tau$ , where  $C_v$ ,  $v$ ,  $l$ , and  $\tau$  are the heat capacity, phonon velocity, mean free path (MFP), and relaxation time. Furthermore, the phonon velocity is often simply replaced by the sound velocity, which is proportional to  $\sqrt{B/\rho}$ , where  $B$  and  $\rho$  are the elastic modulus and mass density of a material. [8] Accordingly, one method to design low lattice thermal conductivity materials is to search for high density materials due to their low sound velocities, such as Bi<sub>2</sub>Te<sub>3</sub>. Besides, complex crystal structural materials also usually have low sound velocities, such as Yb<sub>14</sub>MnSb<sub>11</sub>. [9] The other way is to reduce

the relaxation time by introduction of defects or nano-structures to scatter phonons. [8] Of course, the intrinsic large anharmonic effect (large grüneisen parameters) in a material will also reduce the relaxation time by phonon-phonon scattering. A distinct example is SnSe, in which the large anharmonicity leads to its exceptional low lattice thermal conductivity. [5] However, this is not intuitive without quantitative calculations.

In this work, we predict by first principles calculations that the layered intermetallic  $\text{Na}_2\text{MgSn}$  and  $\text{Na}_2\text{MgPb}$  have very low and anisotropic intrinsic lattice thermal conductivities. Both materials have a very simple layered structure (8 atoms in the unit cell) and a low mass density (2.82 and 4.01 g/cm<sup>3</sup> for  $\text{Na}_2\text{MgSn}$  and  $\text{Na}_2\text{MgPb}$ , respectively). In particular, we propose that  $\text{Na}_2\text{MgSn}$  is a promising room-temperature TE material. An intermetallic is a solid-state compound exhibiting metallic bonding, defined stoichiometry and ordered crystal structure. It is a large material family, which have a wide various crystal structures, ranging from zero to three in dimensionality. Despite of their metallic bonding, some intermetallics are semiconductors, which is the precondition for their TE applications. There are many works about the potential TE intermetallic materials such as  $\text{Mg}_3\text{Sb}_2$  [10–12],  $\text{CaMgSi}$  [13],  $\text{MGa}_3$  (M=Fe, Ru, and Os) [14],  $\text{YbAl}_3$  [15],  $\text{Zn}_4\text{Sb}_3$  [16],  $\text{Al}_2\text{Fe}_3\text{Si}_3$  [17],  $\text{MIn}_3$  (M=Ru and Ir) [18],  $\text{M}_2\text{Ru}$  (M=Al and Ga) [19] and etc. In particular, many half- and full-Heusler compounds, which are magnetic intermetallics, are found to be good TE materials. [20–23]

In 2012, Yamada *et. al.* reported the synthesis, crystal structure, and basic physical properties of hexagonal intermetallic  $\text{Na}_2\text{MgSn}$ . [24] They found that polycrystalline  $\text{Na}_2\text{MgSn}$  is a small band gap semiconductor with a large Seebeck coefficient of +390  $\mu\text{V}/\text{K}$  and an electrical resistivity of about 10 m $\Omega$  cm at 300 K. As a result, the power factor of  $\text{Na}_2\text{MgSn}$  is almost 40% of that of  $\text{Bi}_2\text{Te}_3$ . [24] Two years later, the same group synthesized the similar intermetallic  $\text{Na}_2\text{MgPb}$ , [25] which is a metal with three different phases from 300 to 700 K. In the experiment, the electrical resistivity of  $\text{Na}_2\text{MgPb}$  is much lower than that of  $\text{Na}_2\text{MgSn}$ , which is only 0.4 m $\Omega$  cm at 300 K. From the preliminary experimental results,  $\text{Na}_2\text{MgSn}$  could be a potential TE material. However, the thermal conductivity of  $\text{Na}_2\text{MgSn}$  is not studied yet in both experiments [24, 25] and the following theoretical work. [26]

The rest of the paper is organized as follows. In section II, we will give the computational details about phonon and thermal conductivity calculations. In section III, we will present our main results about phonon dispersions, temperature dependent and accumulated lattice thermal conductivity, group velocity, Grüneisen parameter, phonon lifetime, and Seebeck

coefficient of Na<sub>2</sub>MgSn and Na<sub>2</sub>MgPb. Some comparisons between different TE materials are also given. Finally, a short conclusion is present.

## II. COMPUTATIONAL DETAILS

The structural properties of Na<sub>2</sub>MgSn and Na<sub>2</sub>MgPb are calculated by the Vienna ab-initio simulation package (VASP) [27, 28] based on the density functional theory. The projected augmented wave method [29, 30] and the generalized gradient approximation with the Perdew-Burke-Ernzerhof exchange-correlation functional [31] are used. The plane-wave cutoff energy is set to be 350 eV. Both the internal atomic positions and the lattice constants are allowed to relax until the maximal residual Hellmann-Feynman forces on atoms are smaller than 0.001 eV/Å. An  $8 \times 8 \times 4$  k-mesh was used in the optimization.

Both the second- and third-order interatomic force constants (IFCs) are calculated by the finite displacement method. The second-order IFCs in the harmonic approximation and the phonon dispersions of Na<sub>2</sub>MgSn and Na<sub>2</sub>MgPb are calculated by the Phonopy code. [32] The third-order (anharmonic) IFCs and the lattice thermal conductivity are calculated by the Phono3py code. [33] We use a  $2 \times 2 \times 2$  supercell (64 atoms) for the calculations of the second- and third-order IFCS in Na<sub>2</sub>MgSn and Na<sub>2</sub>MgPb. And a q-mesh of  $20 \times 20 \times 10$  is used for the calculation of lattice thermal conductivity by Phono3py code.

We do not use the crude force constants approximation in the third-order IFCS, although we have checked that a cutoff distance of 4 Å can already obtain a good thermal conductivity. We also checked a larger supercell of  $3 \times 3 \times 2$  in Na<sub>2</sub>MgSn with a cutoff distance of 5 Å, and we found that the thermal conductivity changed little.

The Seebeck coefficients of Na<sub>2</sub>MgSn and Na<sub>2</sub>MgPb are calculated by the BoltzTraP2 program [34] with the Boltzmann transport theory. The electron eigenvalues in the whole Brillouin zone are calculated by the VASP code with the hybrid functional of Heyd-Scuseria-Ernzerhof (HSE06) [35] and spin-orbit coupling. A k-mesh of  $20 \times 20 \times 10$  is used in the calculations of Seebeck coefficient.

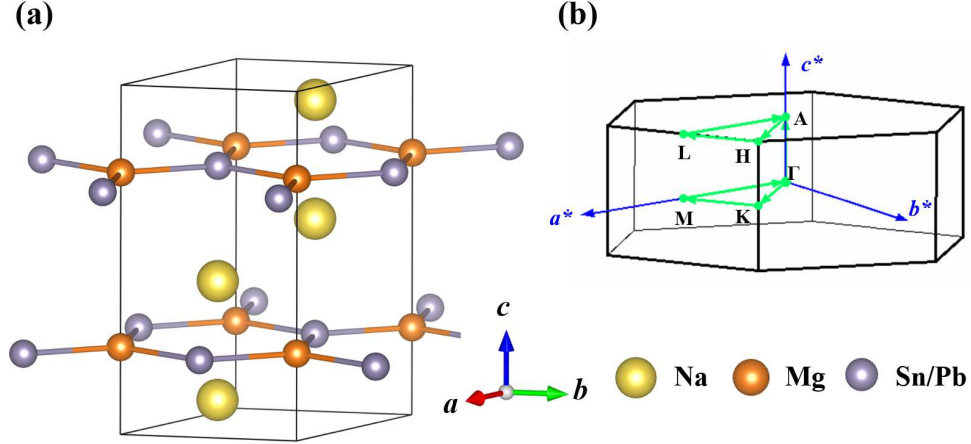


FIG. 1: (Color online) (a) Layered crystal structure and (b) Brillouin zone and high symmetry k-points of hexagonal  $\text{Na}_2\text{MgSn}$  and  $\text{Na}_2\text{MgPb}$ .

TABLE I: Calculated and experimental lattice constants of hexagonal  $\text{Na}_2\text{MgSn}$  and  $\text{Na}_2\text{MgPb}$ .

Material	Method	$a$ (Å)	$c$ (Å)
$\text{Na}_2\text{MgSn}$	present work	5.0825	10.1075
	exp. (293 K) <sup>a</sup>	5.0486	10.0950
	GGA-USP <sup>b</sup>	5.0085	10.1314
$\text{Na}_2\text{MgPb}$	present work	5.1415	10.1873
	exp. (293 K) <sup>c</sup>	5.1102	10.1714

<sup>a</sup> from reference [24]

<sup>b</sup> from reference [26]

<sup>c</sup> from reference [25]

### III. RESULTS AND DISCUSSIONS

#### A. Crystal Structure and Phonon Dispersions

As shown in Fig. 1(a),  $\text{Na}_2\text{MgSn}$  and  $\text{Na}_2\text{MgPb}$  share the same hexagonal crystal structure with the space group of  $P6_3/mmc$  (No. 194). It is noted that  $\text{Na}_2\text{MgPb}$  has three phases from 300 to 700 K. [25] However, from 300 to 500 K,  $\text{Na}_2\text{MgPb}$  and  $\text{Na}_2\text{MgSn}$  have the same hexagonal crystal structure. [24, 25] Mg and Sn (or Pb) atoms lie in the same

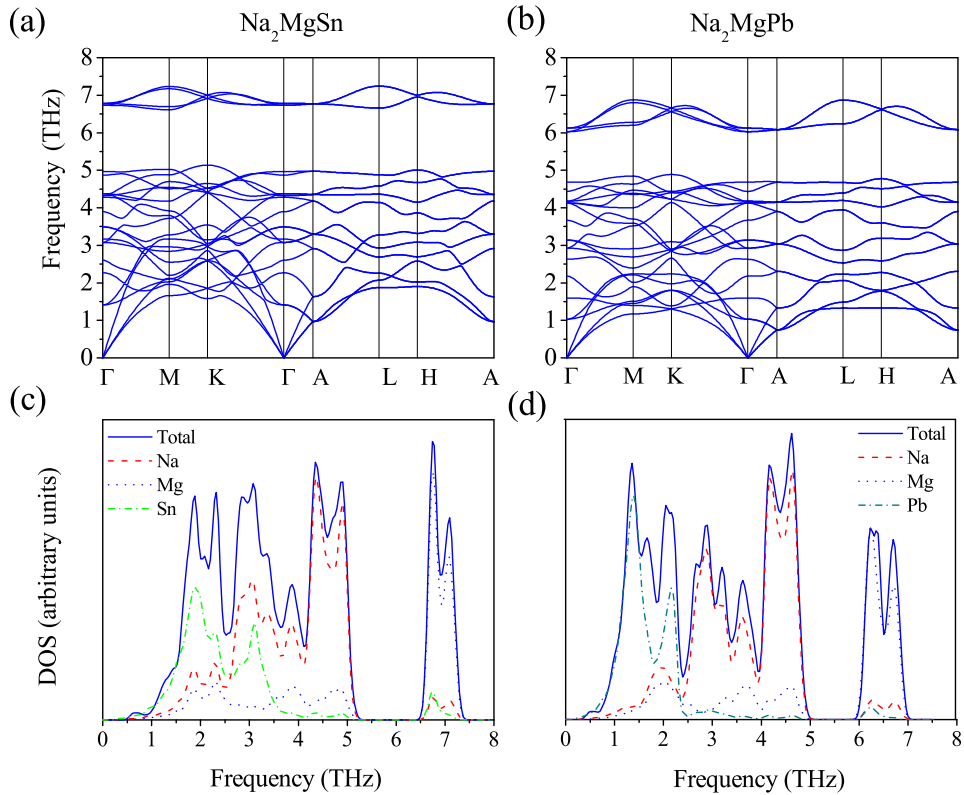


FIG. 2: (Color online) Calculated phonon dispersions and density of states of hexagonal  $\text{Na}_2\text{MgSn}$  (left column) and  $\text{Na}_2\text{MgPb}$  (right column).

plane and form a two-dimensional (2D) honeycomb structure stacking along the  $c$  axis. Two layers of Na atoms are intercalated between the adjacent Mg-Sn (or Mg-Pb) layers. This is quite different from other alkali-intercalated layered materials, such as  $\text{Na}_x\text{CoO}_2$  [36] or  $\text{Na}_x\text{RhO}_2$  [37], in which only one Na layer is intercalated between the adjacent  $\text{CoO}_2$  or  $\text{RhO}_2$  layers. The Brillouin zone and high symmetry k-points of  $\text{Na}_2\text{MgSn}$  and  $\text{Na}_2\text{MgPb}$  are given in Fig. 1(b).

The optimized lattice constants as well as the experimental ones of  $\text{Na}_2\text{MgSn}$  and  $\text{Na}_2\text{MgPb}$  are given in Table I. We find that the theoretical and experimental lattice constants are well consistent to each other, with the largest difference less than 1%. Our calculated lattice constant is also consistent with Wang's calculation by the generalized gradient approximation with the ultra-soft pseudopotentials (GGA-USP). [26]

Based on the optimized structures, the phonon dispersions and density of states (DOS) of  $\text{Na}_2\text{MgSn}$  and  $\text{Na}_2\text{MgPb}$  are calculated by the Phonopy code, given in Fig. 2. It is obvious

TABLE II: Calculated lattice thermal conductivities  $\kappa_a$  and  $\kappa_c$  along  $a$  and  $c$  axes and their average value  $\bar{\kappa}$  of hexagonal  $\text{Na}_2\text{MgSn}$  and  $\text{Na}_2\text{MgPb}$  at 300 K. The unit is  $\text{W}/\text{m}\cdot\text{K}$ .

Material	$\kappa_a$	$\kappa_c$	$\bar{\kappa}$
$\text{Na}_2\text{MgSn}$	1.75	0.80	1.27
$\text{Na}_2\text{MgPb}$	0.51	0.31	0.44

that two materials show very similar phonon dispersions due to the same crystal structures. The highest frequency is about 7.5 and 7.0 THz for  $\text{Na}_2\text{MgSn}$  and  $\text{Na}_2\text{MgPb}$  respectively. There is also a clear band gap from 5 to 6.5 THz for  $\text{Na}_2\text{MgSn}$  and from 5 to 6 THz for  $\text{Na}_2\text{MgPb}$ .

From the phonon DOS in Fig. 2(c) and (d), it is found that the high frequency phonon modes above the band gap are mainly contributed from the vibrations of Mg ions. This feature is same for  $\text{Na}_2\text{MgSn}$  and  $\text{Na}_2\text{MgPb}$ . The main difference in phonon DOS between the two materials is the vibrations of Sn and Pb ions. Due to the larger atomic mass of Pb ions, the vibrational frequencies of Pb ions are mainly below 2.5 THz in  $\text{Na}_2\text{MgPb}$ , while the phonon modes of Sn ions extend from 0 to 4 THz in  $\text{Na}_2\text{MgSn}$ . The vibrations of Na ions are similar in both materials, which spread from 0 to 5 THz. It is also noted that the mid-frequency phonon modes from 2.5 to 5 THz in  $\text{Na}_2\text{MgPb}$  are mainly contributed from the vibrations of Na ions. However, for the phonon modes in the same frequency range in  $\text{Na}_2\text{MgSn}$ , there are also significant contribution from the vibrations of Sn ions. In other words, the vibrations of Na, Mg, and Pb ions in  $\text{Na}_2\text{MgPb}$  are well separated in different frequency regions, while there is a relatively large overlap in  $\text{Na}_2\text{MgSn}$ .

## B. Lattice Thermal Conductivities

Based on the harmonic and anharmonic IFCs, we have calculated the lattice thermal conductivity ( $\kappa_L$ ) by using the Phono3py code. Fig. 3(a) shows the temperature-dependent thermal lattice conductivities along  $a$  and  $c$  axes of  $\text{Na}_2\text{MgSn}$  and  $\text{Na}_2\text{MgPb}$ , while the average ones are also given in Fig. 3(b). It is quite surprising to found that the  $\kappa_L$  of the two intermetallics are very low. As shown in Fig. 3 and Table II, the  $\kappa_L$  of  $\text{Na}_2\text{MgSn}$  is



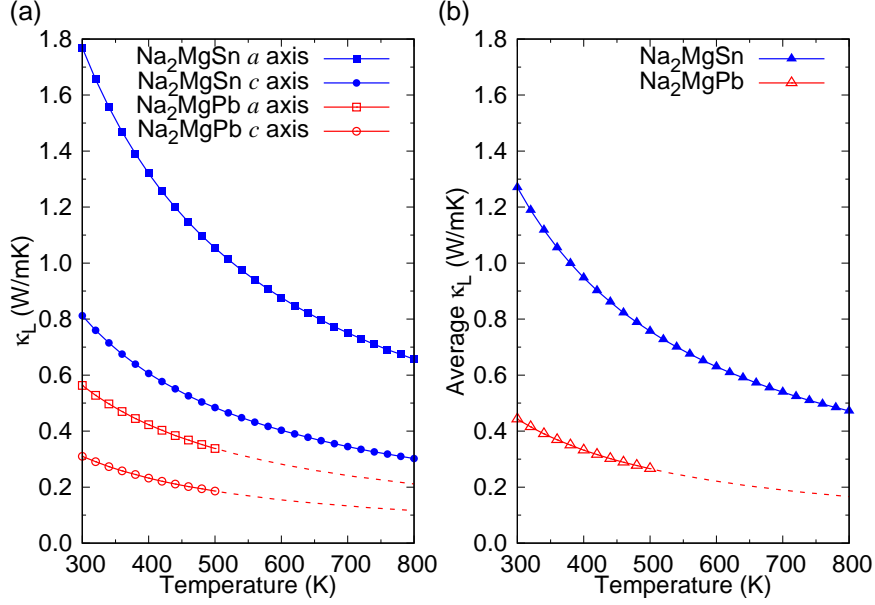


FIG. 3: (Color online) (a) Calculated lattice thermal conductivities and (b) their average values of hexagonal  $\text{Na}_2\text{MgSn}$  and  $\text{Na}_2\text{MgPb}$  from 300 to 800 K. The red dashed lines mean that the high temperature lattice thermal conductivities are calculated based on a low temperature crystal structure of  $\text{Na}_2\text{MgPb}$ .

only 1.75 and 0.80 W/m·K along  $a$  and  $c$  axes at 300 K, while it is even much lower for  $\text{Na}_2\text{MgPb}$ , which is 0.51 and 0.31 W/m·K along  $a$  and  $c$  axes at the same temperature. Specifically, the  $\kappa_L$  along the  $c$  axis in  $\text{Na}_2\text{MgPb}$  even approaches the predicted amorphous limit (0.25 W/m·K), [38] which is extremely low for crystalline solids. The lattice thermal conductivity of  $\text{Na}_2\text{MgSn}$  is comparable with the typical good TE materials, which will be discussed later. While the lattice thermal conductivity of  $\text{Na}_2\text{MgPb}$  is even smaller than that of the recently found best TE material SnSe, which is 0.8, 2.0 and 1.7 W/m·K along  $a$ ,  $b$ , and  $c$  axes at 300 K from the first-principles calculations. [39] It is noted that the lattice thermal conductivity of  $\text{Na}_2\text{MgPb}$  above 500 K is meaningless since  $\text{Na}_2\text{MgPb}$  has different crystal structures above that temperature. However, since we mainly focus on the room temperature behavior of  $\text{Na}_2\text{MgPb}$ , it is not necessary to study its high temperature thermal conductivity.

Furthermore, it is obvious that  $\text{Na}_2\text{MgSn}$  and  $\text{Na}_2\text{MgPb}$  both show an anisotropic lattice thermal conductivities due to their layered crystal structures. However, the ratio of thermal conductivities between the  $a$  and  $c$  directions in both materials is smaller than 2. The

TABLE III: Calculated sound velocities along  $a$  and  $c$  axes of  $\text{Na}_2\text{MgSn}$  and  $\text{Na}_2\text{MgPb}$ . The unit is km/s.

Material	$v_a$	$v_c$
$\text{Na}_2\text{MgSn}$	2.75	2.41
$\text{Na}_2\text{MgPb}$	2.16	1.90

small anisotropy suggests that easily-formed texture structures in layered compounds has not much effect on thermoelectric performance of these compounds.

We also calculated the average lattice thermal conductivity  $\bar{\kappa}$ , defined by the formula  $3/\bar{\kappa} = 2/\kappa_a + 1/\kappa_c$ , shown in Fig. 3(b) and Table II. The average  $\bar{\kappa}$  for  $\text{Na}_2\text{MgSn}$  and  $\text{Na}_2\text{MgPb}$  are 1.27 and 0.44 W/m·K at 300 K respectively.

We then estimate the electronic thermal conductivity ( $\kappa_e$ ) by the Wiedemann-Franz law:  $\kappa_e = LT\sigma$ , where  $L$  is the Lorenz number ( $2.44 \times 10^{-8} \text{ W}\Omega\text{K}^{-2}$ ),  $\sigma$  is the electrical conductivity, and  $T$  is the absolute temperature. According to previous experiments [24, 25], we can obtain the electrical resistivities ( $\rho$ ) of  $\text{Na}_2\text{MgSn}$  and  $\text{Na}_2\text{MgPb}$  are about 10 and 0.4 m $\Omega$  cm at 300 K, respectively. Therefore, the electronic thermal conductivity of  $\text{Na}_2\text{MgSn}$  and  $\text{Na}_2\text{MgPb}$  are estimated to be 0.073 and 1.83 W/m·K, respectively. For the semiconducting  $\text{Na}_2\text{MgSn}$ , its electronic thermal conductivity is much smaller than the lattice one. While for the metallic  $\text{Na}_2\text{MgPb}$ , the electron contributes more thermal conductivity than the lattice one. Of course, it has to be noted that the experimental samples are both polycrystals. No single crystal sample has been reported yet.

The sound velocity is also calculated by the slopes of three acoustic phonon branches near the  $\Gamma$  point. For each directions, the sound velocity is averaged on the two transversal acoustic modes, (TA1 and TA2), and one longitudinal acoustic mode (LA) by the formula:  $3/v_x^3 = 1/v_{x,\text{TA1}}^3 + 1/v_{x,\text{TA2}}^3 + 1/v_{x,\text{LA}}^3$ , where  $x$  means the  $a$  and  $c$  axes. In Table II, we can see that in  $a$  and  $c$  axes, the sound velocities of  $\text{Na}_2\text{MgSn}$  are both higher than those of  $\text{Na}_2\text{MgPb}$ , which can explain why  $\text{Na}_2\text{MgSn}$  has higher lattice thermal conductivities. For both materials, the sound velocity along  $a$  axis is higher than that along  $c$  axis, which can explain the anisotropic lattice thermal conductivities in two materials.

We further plot the directional cumulative lattice thermal conductivity with respect to

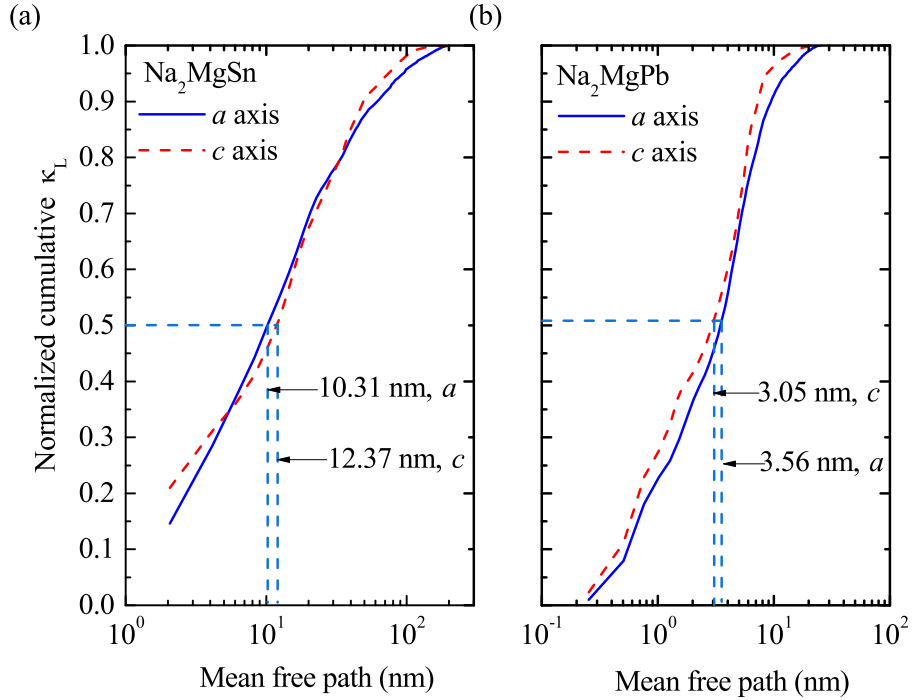


FIG. 4: (Color online) Normalized directional accumulated lattice thermal conductivities of hexagonal (a)  $\text{Na}_2\text{MgSn}$  and (b)  $\text{Na}_2\text{MgPb}$  at 300 K.

the phonon MFP in  $\text{Na}_2\text{MgSn}$  and  $\text{Na}_2\text{MgPb}$  at 300 K in Fig. 4. It is found that the  $\kappa_L$  of  $\text{Na}_2\text{MgSn}$  is mainly dominated by the phonons whose MFPs are less than 100 nm. However, for  $\text{Na}_2\text{MgPb}$ , the  $\kappa_L$  is mostly contributed by the phonons whose MFPs are less than 20 nm. This indicates that the phonon MFP in  $\text{Na}_2\text{MgPb}$  is much shorter than that in  $\text{Na}_2\text{MgSn}$ , leading to a much lower  $\kappa_L$  in  $\text{Na}_2\text{MgPb}$  than that in  $\text{Na}_2\text{MgSn}$ .

We also give the representative MFP (rMFP) for the two materials in Fig. 4. This parameter (rMFP) means that all the phonons whose MFP is shorter than the rMFP will contribute half to the total thermal conductivity. It is clear to see that the rMFP of  $\text{Na}_2\text{MgPb}$  is much shorter than that of  $\text{Na}_2\text{MgSn}$ . For  $\text{Na}_2\text{MgSn}$ , the rMFP along the  $a$  and  $c$  axes are 10.31 and 12.37 nm respectively, while they are only 3.56 and 3.05 nm along the same axes for  $\text{Na}_2\text{MgPb}$ . The rMFP of  $\text{Na}_2\text{MgPb}$  is even a little shorter than the ones of SnSe, which are 4.1, 4.9, and 5.6 nm along  $a$ ,  $b$ , and  $c$  axes at 300 K from the first-principles calculations. [39]

Due to their different MFP, we suggest that for  $\text{Na}_2\text{MgSn}$ , structural engineerings, such as nano-structuring or polycrystalline structures, can be taken to reduce the thermal con-

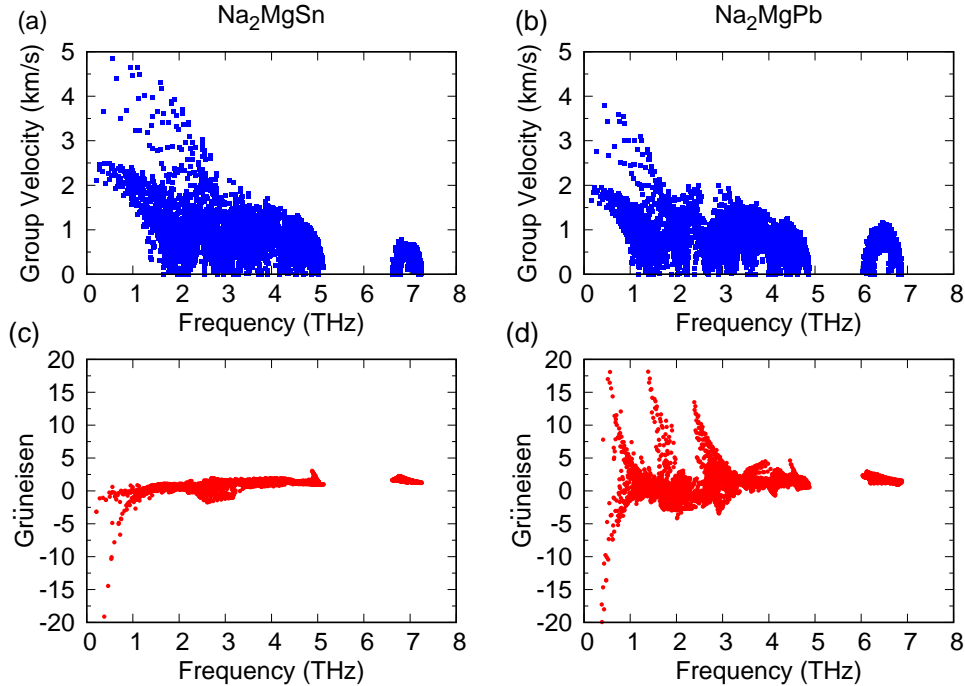


FIG. 5: (Color online) Calculated group velocities and mode-dependent Grüneisen parameters of Na<sub>2</sub>MgSn (left column) and Na<sub>2</sub>MgPb (right column) .

ductivity effectively in experiments, while it would be much ineffective for Na<sub>2</sub>MgPb.

### C. Group velocity and phonon anharmonicity

In order to further understand the intrinsic thermal lattice conductivity and their difference in Na<sub>2</sub>MgSn and Na<sub>2</sub>MgPb, we also calculated their frequency dependent phonon group velocities, mode-dependent Grüneisen parameter, and phonon lifetimes.

In Fig. 5 (a) and (b), we have given the magnitude of frequency dependent phonon group velocities of Na<sub>2</sub>MgSn and Na<sub>2</sub>MgPb. We can see that the group velocities of Na<sub>2</sub>MgPb are only slightly smaller than those of Na<sub>2</sub>MgSn, which is difficult to explain the significant difference of  $\kappa_L$  of the two materials. Therefore, we need to further study their anharmonic effect: the Grüneisen parameters. In general, larger Grüneisen parameter means larger anharmonicity of the material and lower lattice thermal conductivity. In Fig. 5 (c) and (d), the magnitude of Grüneisen parameters for Na<sub>2</sub>MgPb is obviously much larger than that of Na<sub>2</sub>MgSn, which means that Na<sub>2</sub>MgPb has a much stronger phonon anharmonicity. In other words, stronger phonon scattering leads to lower lattice thermal conductivity in

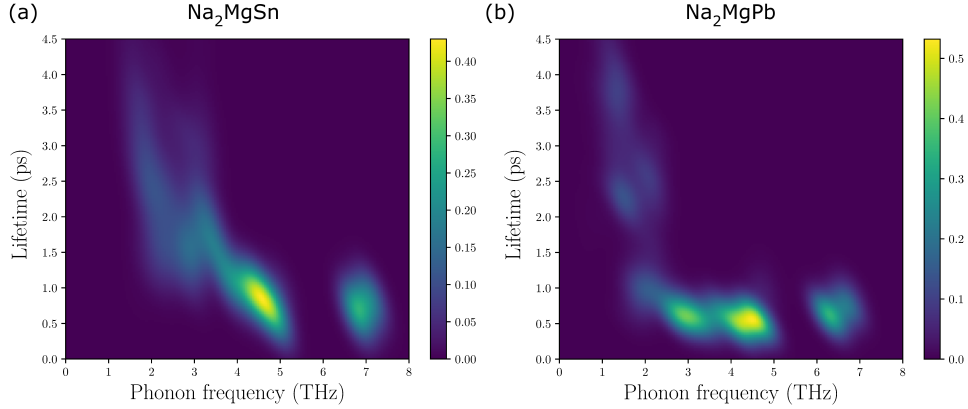


FIG. 6: (Color online) Calculated phonon lifetimes of (a)  $\text{Na}_2\text{MgSn}$  and (b)  $\text{Na}_2\text{MgPb}$  at 300 K. The color in the figure represents the phonon density. Brighter color means a higher phonon density.

$\text{Na}_2\text{MgPb}$  than that in  $\text{Na}_2\text{MgSn}$ .

The frequency-dependent phonon lifetimes of  $\text{Na}_2\text{MgSn}$  and  $\text{Na}_2\text{MgPb}$  are also calculated by the Phono3py code from third-order anharmonic IFCs, plotted in Fig. 6. The color bar in Fig. 6 represent the density of phonon modes. In general, we found that the phonon lifetimes of both materials are very short, roughly ranging from 0.4 to 4.5 ps, which are much smaller than those of SnSe (from 0 to 30 ps). [39] In detail, we can see that in the low frequency region below 2.5 THz, the phonon lifetimes of both materials show a large broad distribution with a maximal value about 4.5 ps. The lifetimes of the high frequency phonons (above the band gap) of the two materials are also similar with a narrow distribution from 0.5 to 1.0 ps. The major differences between the two materials are from the mid-frequency phonons, i.e. from 2.5 to 5 THz. In this region, the phonons of  $\text{Na}_2\text{MgSn}$  have a relatively broader distribution from 0 to 1.5 ps, while in  $\text{Na}_2\text{MgPb}$ , the phonons have much smaller lifetimes, located from 0.4 to 0.8 ps. Therefore, we conclude that the phonon modes between 2.5 to 5 THz scatter much stronger in  $\text{Na}_2\text{MgPb}$  than those in  $\text{Na}_2\text{MgSn}$ , which is the main reason for the lower lattice thermal conductivity in  $\text{Na}_2\text{MgPb}$  than that of  $\text{Na}_2\text{MgSn}$ .

#### D. Seebeck coefficient

In order to estimate the  $ZT$  of  $\text{Na}_2\text{MgPb}$ , we have also calculated the Seebeck coefficient of two materials, shown in Fig. 7. The electron band structure calculations indicate that

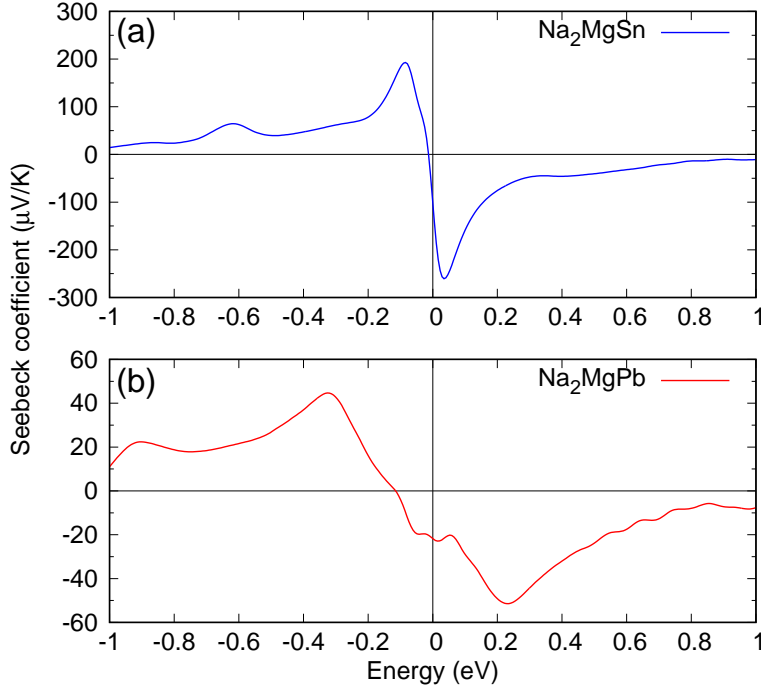


FIG. 7: (Color online) Calculated Seebeck coefficient of (a)  $\text{Na}_2\text{MgSn}$  and (b)  $\text{Na}_2\text{MgPb}$  at 300 K. The Fermi energy is set to 0.

$\text{Na}_2\text{MgSn}$  is a small gap (about 0.18 eV) semiconductor and  $\text{Na}_2\text{MgPb}$  is a semi-metal. In Fig. 7(a), the maximal absolute Seebeck coefficient of  $\text{Na}_2\text{MgSn}$  at 300 K is about 250  $\mu\text{V}/\text{K}$ , which is lower than the experimental value (390  $\mu\text{V}/\text{K}$ ). This is possibly because that the experimental  $\text{Na}_2\text{MgSn}$  is a polycrystalline sample. In Fig. 7(b), it is natural to find that the Seebeck coefficient of metallic  $\text{Na}_2\text{MgPb}$  is quite low. At the Fermi energy, its Seebeck coefficient is about -22  $\mu\text{V}/\text{K}$ .

### E. Discussion

Now, we compare some theoretical physical properties of  $\text{Na}_2\text{MgSn}$  and  $\text{Na}_2\text{MgPb}$  with other well-known TE materials, such as SnSe, SnS,  $\text{Bi}_2\text{Te}_3$ , and PbTe, shown in Table IV. It is found that  $\text{Na}_2\text{MgSn}$  and  $\text{Na}_2\text{MgPb}$  have comparable lattice thermal conductivities as those TE materials. The main difference is that  $\text{Na}_2\text{MgSn}$  and  $\text{Na}_2\text{MgPb}$  have a much smaller mass density, a smaller bulk modulus, and a relatively higher sound velocity. In particular, the mass density of  $\text{Na}_2\text{MgSn}$  is less than half of the SnSe's, while they almost have the same lattice thermal conductivities. This is a quite unique behavior in low  $\kappa$

TABLE IV: Comparison of theoretical lattice thermal conductivity ( $\kappa_L$ ), mass density ( $\rho$ ), bulk modulus ( $B$ ), sound velocity ( $v$ ), and rMFP, and maximal phonon lifetime ( $\tau$ ) of Na<sub>2</sub>MgSn and Na<sub>2</sub>MgPb at 300 K with other TE materials. All physical quantities except the mass density are theoretical ones. The data of Na<sub>2</sub>MgSn and Na<sub>2</sub>MgPb is from the present work. The (a), (b), and (c) in the table indicates the  $a$ ,  $b$ , and  $c$  axes respectively.

Material	$\kappa_L$ (W/m·K)	$\rho$ (g/cm <sup>3</sup> )	$B$ (GPa)	$v$ (km/s)	rMFP (nm)	$\tau$ (ps)
Na <sub>2</sub> MgSn	1.75(a)/0.80(c)	2.82 [24]	30.6	2.75(a)/2.41(c)	10.31(a)/12.37(c)	$\sim 4.5$
Na <sub>2</sub> MgPb	0.51(a)/0.31(c)	4.01 [25]	27.0	2.16(a)/1.90(c)	3.56(a)/3.05(c)	$\sim 4.5$
SnSe [39]	0.8(a)/2.0(b)/1.7(c)	$\sim 6.1$ [45]	39.4	0.40(a)/0.63(b)/0.58(c)	5.6(a)/4.9(b)/4.1(c)	$\sim 30$
SnS [39]	0.9(a)/2.3(b)/1.6(c)	5.1 [46]	41.6	0.44(a)/0.71(b)/0.60(c)	4.3(a)/5.2(b)/4.0(c)	$\sim 30$
Bi <sub>2</sub> Te <sub>3</sub>	1.2(a)/0.4(c) [47]	7.88 [48]	36.4 [48]	1.68(a)/1.79(c) [49]	1.5(a) [47]	
PbTe	2.1 [50]	8.24 [51]	45.51 [52]	1.98 [52]	6 [50]	$\sim 100$ [50]

materials. In spite of the very low mass density and high sound velocity, Na<sub>2</sub>MgSn and Na<sub>2</sub>MgPb show a very low lattice thermal conductivity due to their large anharmonicity. From Table IV, we can see that the maximal lifetime of Na<sub>2</sub>MgSn and Na<sub>2</sub>MgPb is much smaller than those of SnSe, SnS, Bi<sub>2</sub>Se<sub>3</sub>, and PbTe. We think the large anharmonicity is probably due to the Na intercalated layered structures. In Na<sub>2</sub>MgSn and Na<sub>2</sub>MgPb, there are two layers of Na ions loosely confined between adjacent Mg-Sn (or Mg-Pb) layers. The possible rattling modes of the Na ions could suppress the lattice thermal conductivity, as been found in some cage structure materials, such as Ba<sub>8</sub>Ga<sub>16</sub>Ge<sub>30</sub>[40] and layered structure materials, such as Na <sub>$x$</sub> CoO<sub>2</sub>. [41]

Finally, we can compare some experimental properties of Na<sub>2</sub>MgSn and Na<sub>2</sub>MgPb with other TE materials, as shown in Table V. It is found that Na<sub>2</sub>MgSn has a high Seebeck coefficient at room temperatures, which is higher than those of Bi<sub>2</sub>Te<sub>3</sub> and PbTe, but lower than those of SnSe and SnS. It also has a good electric conductivity, which is much higher than those of SnSe and SnS, but lower than those of Bi<sub>2</sub>Te<sub>3</sub> and PbTe. Based on these experimental data and our calculated average total thermal conductivity, we can estimate that the  $ZT$  of Na<sub>2</sub>MgSn is about 0.34 at 300 K, which is comparable with the  $ZT$  values of

TABLE V: Comparison of experimental electric conductivity ( $\sigma$ ), absolute Seebeck coefficient ( $S$ ), total thermal conductivity ( $\kappa$ ), and figure of merit  $ZT$  of  $\text{Na}_2\text{MgSn}$  and  $\text{Na}_2\text{MgPb}$  at 300 K with other TE materials. The values with \* are theoretical ones or estimated ones based on the theoretical results. In the table, only SnSe sample is a single crystal.

Material	$\sigma$ ( $\Omega^{-1} \text{ cm}^{-1}$ )	$S$ ( $\mu\text{V}/\text{K}$ )	$\kappa$ ( $\text{W}/\text{m}\cdot\text{K}$ )	$ZT$
$\text{Na}_2\text{MgSn}$ [24]	100	390	1.343*	0.34*
$\text{Na}_2\text{MgPb}$ [25]	2500	22*	2.27*	0.016*
SnSe [5]	1.6(a)/10(b)/10.3(c)	542(a)/522(b)/515(c)	0.46(a)/0.7(b)/0.68(c)	0.03(a)/0.12(b)/0.12(c)
SnS [53]	0.001	400	1.25	$\sim 0$
$\text{Bi}_2\text{Te}_3$ [54]	962	226	1.47	1.003
PbTe [51]	200	192	1.7	0.13

$\text{Bi}_2\text{Te}_3$  and PbTe, but much higher than those of SnSe and SnS at the same temperatures. We also note that in a polycrystalline sample, the thermal conductivity should be greatly suppressed usually. For example, the experimental thermal conductivity of polycrystalline  $\text{ZrTe}_5$  is only 2.2 W/m·K at room temperatures,[42] which is much lower than the experimental and theoretical values of single crystalline  $\text{ZrTe}_5$  (about 8 W/m·K at 300 K).[43, 44] Therefore, we expect that the thermal conductivity of polycrystalline  $\text{Na}_2\text{MgSn}$  should be much smaller than our calculated value and its  $ZT$  could be possibly much larger than 0.34 at 300 K. It is also noted that the SnSe and SnS have the best performance at high temperatures (more than 700 K), while we believe that  $\text{Na}_2\text{MgSn}$  would have the highest  $ZT$  near the room temperatures due to its small band gap.

On the other hand, although  $\text{Na}_2\text{MgPb}$  has an ultra-low lattice thermal conductivity, its total  $\kappa_L$  (about 2.27 W/m·K) is not small due to its metallicity. In experiment, Yamada *et al* have found a very small electrical resistivity of polycrystalline  $\text{Na}_2\text{MgPb}$  (only 0.4 m $\Omega$  cm at 300 K). Combined with our theoretical Seebeck coefficient, we can estimate the  $ZT$  of  $\text{Na}_2\text{MgPb}$  is very small, which is only about 0.016 at 300 K, as shown in Table V. Therefore, metallic  $\text{Na}_2\text{MgPb}$  could not be a good TE material.



## IV. CONCLUSIONS

We have studied the lattice thermal conductivities and thermoelectric properties of  $\text{Na}_2\text{MgSn}$  and  $\text{Na}_2\text{MgPb}$  based on the density functional theory and linearized Boltzmann equation. Despite of their very low mass density and simple crystal structure, both materials show very low lattice thermal conductivities, compared with other well-known TE materials. The lattice thermal conductivities along  $a$  and  $c$  axes of  $\text{Na}_2\text{MgSn}$  are 1.75 and 0.80 W/m·K respectively at 300 K, while they are much lower in  $\text{Na}_2\text{MgPb}$ , which are 0.51 and 0.31 W/m·K along  $a$  and  $c$  axes at the same temperature. The main reason for the low thermal conductivity is due their large anharmonic effect.

$\text{Na}_2\text{MgPb}$  could not be a good TE material due to its metallicity. However, we predict that  $\text{Na}_2\text{MgSn}$  is a potential room-temperature TE material with a considerable large  $ZT$  of 0.34 at least. Since the intermetallic is a large material family, our work can possibly stimulate further experimental and theoretical works about the thermoelectric research in simple layered intermetallic compounds.

*Note Added:* During the preparation of this manuscript, B. Peng *et al.* predicted that  $\text{Na}_2\text{MgPb}$  is a Dirac semi-metal, while  $\text{Na}_2\text{MgSn}$  is a trivial indirect semiconductor with a small band gap of about 0.2 eV. [55]

### Acknowledgments

We thank Dr. Yang Han for invaluable discussions. This work is supported by the National Key R&D Program of China (2016YFA0201104) and the National Science Foundation of China (Nos. 91622122 and 11474150). The use of the computational resources in the High Performance Computing Center of Nanjing University for this work is also acknowledged.

- 
- [1] G. J. Snyder and E. S. Toberer, *Nat. Mater.* **7**, 105 (2008).
  - [2] M. Zebarjadi, K. Esfarjani, M. S. Dresselhaus, Z. F. Ren, and G. Chen, *Energ. Environ. Sci.* **5**, 5147 (2012).
  - [3] F. J. DjSalvo, *Science* **285**, 703 (1999).

- [4] J. P. Heremans, V. Jovovic, E. S. Toberer, A. Saramat, K. Kurosaki, A. Charoenphakdee, S. Yamanaka, and G. J. Snyder, *Science* **321**, 554 (2008).
- [5] L. D. Zhao, S. H. Lo, Y. Zhang, H. Sun, G. Tan, C. Uher, C. Wolverton, V. P. Dravid, and M. G. Kanatzidis, *Nature* **508**, 373 (2014).
- [6] C. Chang, M. Wu, D. He, Y. Pei, C.F. Wu, X. Wu, H. Yu, F. Zhu, K. Wang, Y. Chen, L. Huang, J. F. Li, J. He, and L. D. Zhao, *Science* **360**, 778 (2018).
- [7] G. A. Slack, *CRC handbook of Thermoelectrics*, page 407-440 (edited by D. M . Rowe, 1995).
- [8] E. S. Toberer, A. Zevalkink, and G. J . Snyder, *J. Mater. Chem.* **21**, 15843 (2011).
- [9] S. R. Brown, S. M. Kauzlarich, F. Gascoin, and G. J. Snyder, *Chem. Mater.* **18**, 1873 (2006).
- [10] W. Peng, G. Petretto, G. M. Rignanese, G. Hautier, and A. Zevalkink, arXiv 1804.01517v1 (2018).
- [11] C. L. Condon, S. M. Kauzlarich, F. Gascoin, and G. J. Snyder, *J. Solid State Chem.* **179**, 2252 (2006).
- [12] A. Bhardwaj, A. Rajput, A. K. Shukla, J. J. Pulikkotil, A. K. Srivastava, A. Dhar, Govind Gupta, S. Auluck, D. K. Misra, and R. C. Budhani, *RSC Adv.* **3**, 8504 (2013).
- [13] N. Miyazaki, N. Adachi, Y. Todaka, H. Miyazaki, and Y. Nishino, *J. Alloys Compd.* **691**, 914 (2017).
- [14] Y. Amagai, A. Yamamoto, T. Lida, and Y. Takanashi, *J. Appl. Phys.* **96**, 5644 (2004).
- [15] J. Liang, D. Fan, P. Jiang, H. Liu, and W. Zhao, *Intermetallics*, **87**, 27 (2017).
- [16] R. Carlini, D. Marre, I. Pallecchi, R. Ricciardi, and G. Zanicchi, *Intermetallics*, **45**, 60 (2014).
- [17] Y. Takagiwa, Y. Isoda, M. Goto, and Y. Shinohara, *J. Therm. Anal. Calorim.* **131**, 281 (2018).
- [18] N. Haldolaarachchige, W. A. Phelan, Y. M. Xiong, R. Jin, J. Y. Chan, S. Stadler, and D. P. Young, *J. Appl. Phys.* **113**, 908 (2013).
- [19] Y. Takagiwa, Y. Matsubayashi, A. Suzumura, J. T. Okada, and K. Kimura, *Mater. Trans.* **51**, 988 (2010).
- [20] W. G. Zeier, J. Schmitt, G. Hautier, U. Aydemir, Z. M. Gibbs, C. Felser, and G. J. Snyder, *Nature Reviews Materials*, **1**, 16032 (2016).
- [21] J. He, M. Amsler, Y. Xia, S. S. Naghavi, V. I. Hegde, S. Hao, S. Goedecker, V. Ozoliņš, and C. Wolverton, *Phys. Rev. Lett.*, **117**, 046602 (2016).
- [22] L. Huang, Q. Zhang, B. Yuan, X. Lai, X. Yan, and Z. Ren, *Mater. Res. Bull.* **76**, 107 (2016).
- [23] F. Casper, T. Graf, S. Chadov, B. Balke, and C. Felser, *Semicond. Sci. Technol.*, **27**, 063001

- (2012).
- [24] T. Yamada, V. L. Deringer, R. Dronskowski, and H. Yamane, *Inorg. Chem.* **51**, 4810 (2012).
- [25] T. Yamada, T. Ikeda, R. P. Stoffel, V. L. Deringer, R. Dronskowski, and H. Yamane, *Inorg. Chem.* **53**, 5253 (2014).
- [26] Y. F. Wang, Q. L. Xia, L. X. Pan, and Y. Yu, *Trans. Nonferrous Met. Soc. China* **24**, 1853 (2014).
- [27] G. Kresse and J. Furthmüller, *Comput. Mater. Sci.* **6**, 15 (1996).
- [28] G. Kresse and J. Furthmüller, *Phys. Rev. B* **54**, 11169 (1996).
- [29] P. E. Blöchl, *Phys. Rev. B* **50**, 17953 (1994).
- [30] G. Kresse and D. Joubert, *Phys. Rev. B* **59**, 1758 (1999).
- [31] J. P. Perdew, K. Burke, and M. Ernzerhof, *Phys. Rev. Lett.* **77**, 3865 (1996).
- [32] A. Togo and I. Tanaka, *Scr. Mater.* **108**, 1 (2015).
- [33] A. Togo, L. Chaput, and I. Tanaka, *Phys. Rev. B* **91**, 094306 (2015).
- [34] G. K. H. Madsen, J. Carrete, and M. J. Verstraete, *Comput. Phys. Commun.* **231**, 140 (2018).
- [35] J. Heyd, G. E. Scuseria, and M. Ernzerhof, *J. Chem. Phys.* **124**, 219906 (2006).
- [36] I. Terasaki, Y. Sasago, and K. Uchinokura, *Phys. Rev. B* **56**, R12685 (1997).
- [37] B. B. Zhang, C. Wang, S. T. Dong, Y. Y. Lv, L. Y. Zhang, Y. D. Xu, Y. B. Chen, J. Zhou, S. H. Yao, and Y. F. Chen, *Inorg. Chem.* **57**, 2730 (2018).
- [38] D. G. Cahill, S. K. Watson, and R. O. Pohl, *Phys. Rev. B* **46**, 6131 (1992).
- [39] R. Guo, X. Wang, Y. Kuang, and B. Huang, *Phys. Rev. B* **92**, 115202 (2015).
- [40] M. Christensen, A. B. Abrahamsen, N. B. Christensen, F. Juranyi, N. H. Andersen, K. Lefmann, J. Andreasson, C. R. H. Bahl, and B. B. Iversen, *Nat. Mater.* **7**, 811 (2008).
- [41] D. J. Voneshen, K. Refson, E. Borissenko, M. Krisch, A. Bosak, A. Piovano, E. Cemal, M. Enderle, M. J. Gutmann, M. Hoesch, M. Roger, L. Gannon, A. T. Boothroyd, S. Uthayakumar, D. G. Porter, and J. P. Goff, *Nat. Mater.* **12**, 1028 (2013).
- [42] M. K. Hooda and C. S. Yadav, *Appl. Phys. Lett.* **111**, 053902 (2017).
- [43] B. M. Zawilski, R. T. Littleton IV, and Terry M. Tritt, *Appl. Phys. Lett.* **77**, 2319 (2000).
- [44] C. Wang, H. F. Wang, Y. B. Chen, S. H. Yao, and J. Zhou, *J. Appl. Phys.* **123**, 175104 (2018).
- [45] P. C. Wei, S. Bhattacharya, J. He, S. Neeleshwar, R. Podila, Y. Y. Chen, and A. M. Rao, *Nature*, **539**, E1 (2016).
- [46] P. K. Nair, M. T. S. Nair, and J. Campos, *J. Electrochem. Soc.* **140**, 539 (1993).

- [47] O. Hellman and D. A. Broido, *Phys. Rev. B* **90**, 134309 (2014).
- [48] A. Gaul, Q. Peng, D. J. Singh, G. Ramanath, and T. Borca-Tasciuc, *Phys. Chem. Chem. Phys.* **19**, 12784 (2017).
- [49] X. Chen, D. Parker, and D. J. Singh, *Phys. Rev. B* **87**, 045317 (2013).
- [50] Z. Tian, J. Garg, K. Esfarjani, T. Shiga, J. Shiomi, and G. Chen, *Phys. Rev. B* **85**, 184303 (2012).
- [51] Y. L. Pei and Y. Liu, *J. Alloys Compd.* **514**, 40 (2012).
- [52] E. Joseph and Y. Amouyal, *J. Electron. Mater.* **44**, 1460 (2014).
- [53] Q. Tan, L. D. Zhao, J. F. Li, C. F. Wu, T. R. Wei, Z. B. Xing, and M. G. Kanatzidis, *J. Mater. Chem. A* **2**, 17302 (2014).
- [54] N. Gothard, X. Ji, J. He, and Terry M. Tritt, *J. Appl. Phys.* **103**, 054314 (2008).
- [55] B. Peng, C. Yue, H. Zhang, Z. Fang, and H. M. Weng, *arXiv:1807.01434* (2018).